Experimental Investigation of MISO Vehicular Visible Light Communication under Mobility Conditions

Daniel K. Tettey[1,2], Bismillah Nasir Ashfaq[1,2], Mohammed Elamassie[2] and Murat Uysal[3,2]
[1]Research and Development, Ford Otosan, Istanbul, Turkey
[2]Department of Electrical and Electronics Engineering, Özyeğin University, Istanbul, Turkey.
[3]Engineering Division, New York University Abu Dhabi, Abu Dhabi, UAE.

***Abstract*—Visible light communication (VLC) has attracted attention as a candidate connectivity solution for future intelligent transportation systems by leveraging existing vehicle headlights and taillights as wireless transmitters. In this paper, we present an experimental investigation of an MISO vehicular VLC system in which the two headlights of a vehicle simultaneously transmit the same safety messages to another vehicle with a single photodetector receiver installed at the back of the vehicle. It is expected that the two transmission paths will provide link diversity to improve the communication reliability. Our experimental findings demonstrate that error-free communication using the OOK scheme is possible beyond a 40 m transmission range when the vehicles are in perfect alignment. In our mobility tests, where both vehicles were moving at a speed of approximately 20 km/h with a separation distance of 8-10 m between the vehicles, we achieved an average PDR of 89.58% for 2 × 1 MISO configuration, which was reduced to 81.05% when a single headlight was used for transmission in SISO configuration.**

***Index Terms*—Intelligent Transportation System, Vehicular Visible Light Communication, Software-Defined Radio, 6G, USRP**

I. Introduction

According to the World Health Organization (WHO) report, approximately 1.3 million people die each year due to road traffic crashes, and more than half of all road traffic deaths are among vulnerable road users: pedestrians, cyclists, and motorcyclists [1]. To improve road safety and enhance traffic efficiency, the automotive industry and governments are working towards the adoption of Intelligent Transportation Systems (ITS), where vehicles can coordinate to share safety-critical messages [2], [3]. ITSs require ultra-reliable low-latency wireless communications from vehicle-to-vehicle (V2V), infrastructure-to-vehicle (I2V), and vehicle-to-pedestrian (V2P) to realize their full potential.

The imminent scarcity of the radio frequency (RF) spectrum, possible congestion in high-density vehicular traffic scenarios, and the ubiquity of light-emitting diodes (LEDs) in the exterior lighting of recent vehicles and road-side infrastructures has prompted the consideration of VLC as an alternative and/or complementary connectivity solution to RF systems in vehicular communications [4] - [7]. Unlike RF, vehicular VLC transmission links are usually directed, making the communication dependent upon the existence of line-of-sight (LOS) between the LED emitter and optical sensor [8]. Consequently, only light beams within the field-of-view (FOV) of the receiver can be detected. As a result, a wide FOV receiver is required to receive signals from multiple directions, particularly in mobility conditions, as encountered in dynamic vehicular environments. However, the use of a wide FOV to allow for receiving optical signals from multiple directions is a double-edged approach to the problem, as it degrades the communication performance by increasing optical interference and background noise. Furthermore, although most indoor LEDs have a Lambertian pattern, vehicular headlights exhibit an asymmetrical intensity distribution [9], which mainly aims to illuminate the road. The utilization of vehicular headlights, therefore, brings additional challenges to a vehicular VLC system that is supposed to work in highly dynamic and mobile conditions.

Initial studies on vehicular VLC systems assumed perfect alignment between the LED emitter and photoreceiver [10]-[13]. Such an idealistic scenario cannot be guaranteed under vehicle mobility as it rarely exists. To address the challenges posed by mobility in vehicular environments, the authors of [14] and [15] proposed a tracking mechanism to detect the orientation of an LED transmitter and subsequently adjust the orientation of the photodiode receiver to improve the received signal strength. In [14], the authors employed a low-cost camera to receive LED position information, which was subsequently used to control the orientation of the photodiode receiver using a motor. Similarly, the work in [15] also utilized the setup in [14] with additional components, such as galvanometer mirrors, to track the LED transmitter. These solutions are complex because they involve additional components and limit real implementation in future ITS.

The use of multiple photodetectors (PDs) has also been proposed to combat VLC link misalignment [13], [16], [17]. The work in [17] investigated the use of multiple PDs through an extensive simulation study, with the aim of achieving omnidirectional coverage under various driving and mobility conditions. There have also been some experimental efforts highlighting the benefits of multiple PDs in vehicular VLC. In particular, the authors of [13] implemented a vehicular VLC system using software-defined radio platforms. Their implementation employed two PDs: one positioned at the left-back and the other at left-side of the vehicle. An outdoor

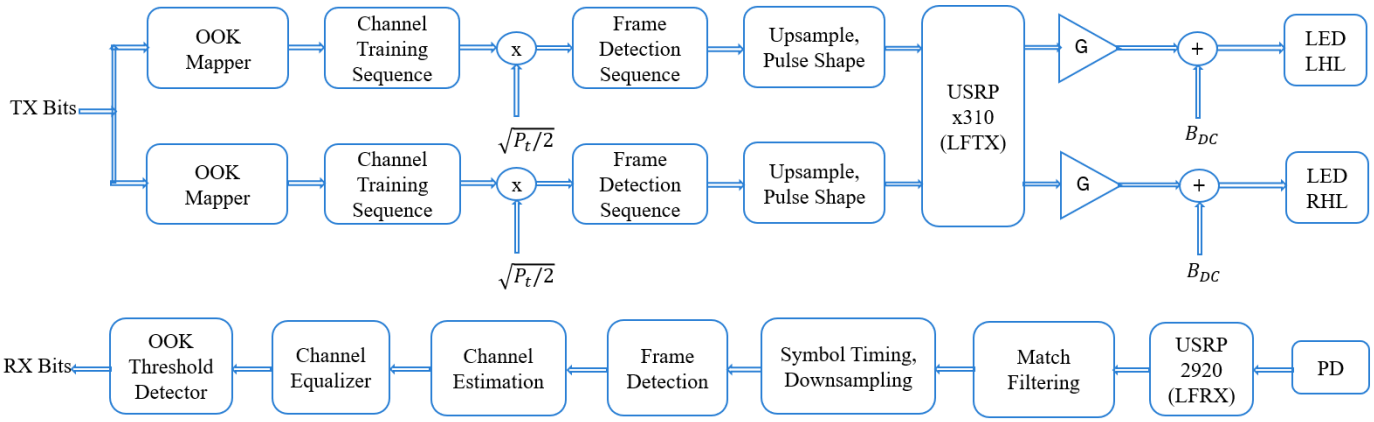

Fig. 1: 2 x 1 MISO vehicular VLC system model

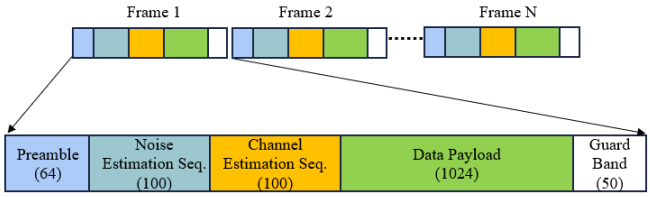

Fig. 2: Frame structure

experiment demonstrated that a vehicular VLC link could be maintained while driving on a curved road with a PD located on the side of the vehicle. In [18], authors conducted the first-ever real-world mobility tests of vehicle-to-vehicle VLC system employing single taillight as wireless transmitter and single PD as receiver. The above-referenced experimental studies have employed a single LED headlight or taillight as the optical wireless transmitter for data transmission. It is expected that employing both headlights or taillights of a vehicle in 2 × 1 MISO configuration with repetition coding will improve the link reliability under mobility conditions owing to the availability of multiple transmission paths to the PD.

In this study, we use an experimental approach to investigate an MISO vehicular VLC system that leverages the two headlights of a vehicle to simultaneously transmit the same message to another vehicle. To the best of the authors' knowledge, this work is the first to experimentally investigate an MISO vehicular VLC system under vehicle mobility conditions.

The remaining sections of the paper is organized as follows: Section II presents the system model, Section III describes our experimental set-up, Section IV details the measurement results and discussions, and Section V concludes the paper.

II. System Model

We consider a 2 × 1 MISO vehicular VLC system where both headlights (BHL) of a following vehicle are used to transmit the same messages simultaneously to a single PD at the back of a preceding vehicle. The system model for this scenario is shown in Fig. 1. The transmit-frame structure is illustrated in Fig. 2. Each frame transmitted consists of a preamble used for start-of-frame detection, an all-zero sequence for noise estimation, and an all-one sequence as training symbols for channel estimation. It is assumed that the data payload to be transmitted consists of safety-critical messages obtained from the vehicle's Controller Area Network (CAN) bus. These messages are modulated using an on-off keying (OOK) scheme and transmitted after the channel estimation sequence, as depicted in the frame structure. A guard band consisting of zeros is inserted at the end of each frame.

Now, let assume $s(i)$ is the i^{th} transmitted symbol and $i = 1, 2, ..., L$. The electrical waveform that drives a single LED headlight can be expressed as

$$w(t) = G\sqrt{\frac{P_t}{2}} \sum_{i=0}^{L-1} s(i) g_T(t - iT_s) + B_{DC} \quad (1)$$

where $G, P_t, g_T(t), T_s, B_{DC}$ and L are the amplification gain, average electrical transmit power, transmit pulse shaping filter, symbol period, direct current (DC) bias and message length respectively. The DC bias is used to shift the communication signal to the linear region of the LED. The electrical waveform, $w(t)$, is used to modulate both LED headlights of the following vehicle for transmission through the optical channel to the leading vehicle.

On the receiver side, a single PD converts the optical signal into an electrical signal. The received electrical signal after sampling feeds into a matched filter. After the matched filtering operation, the received electrical waveform from both headlights considering a 2 x 1 MISO configuration is expressed as

$$r(t) = [R\mu w(t) * l(t) * (h_1(t) + h_2(t)) + n(t)] * g_R(t) \quad (2)$$

where, '$*$' is the convolution operator, μ is the electro-optical conversion ratio of LED, R is responsivity of the PD, $l(t)$ is the impulse response of the LED, $g_R(t)$ is the matched filter, $h_1(t)$ and $h_2(t)$ are optical DC channel coefficient from the LED left headlight (LHL) and right headlight (RHL) respectively and

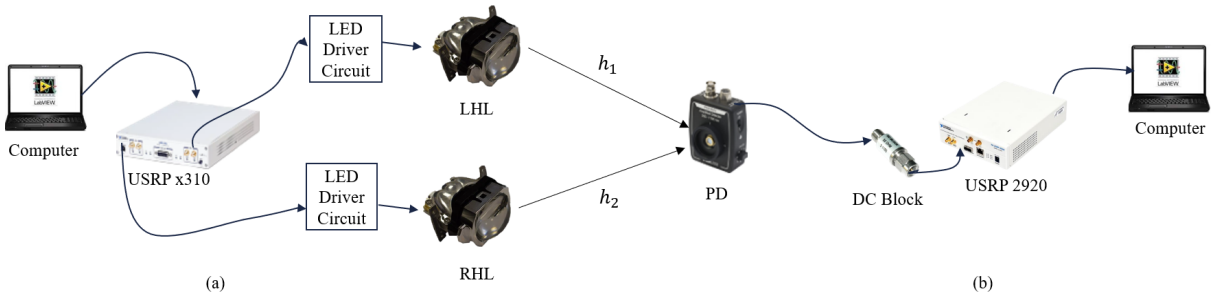

Fig. 3: Block diagram of MISO vehicular VLC set-up (a) transmitter (following vehicle) and (b) receiver (leading vehicle)

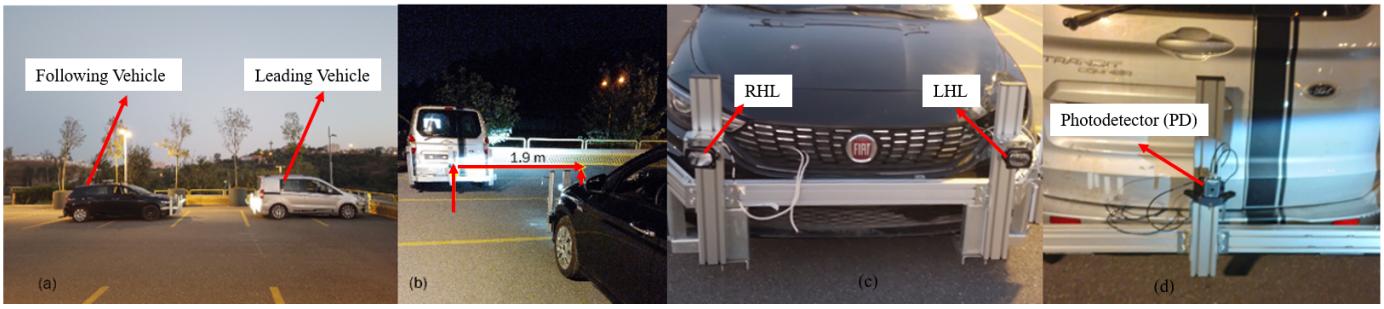

Fig. 4: (a) Both vehicles aligned (b) 1.9 m lateral shift between both vehicles (c) Both LHL and RHL attached to following vehicle at a height of 70 cm from ground and (d) PD attached to leading vehicle at a height of 60 cm from ground.

$n(t)$ is additive white Gaussian noise which models all noise sources in the system. Substituting (1) into (2) and simplifying further yields,

$$r(t) = \left[\sum_{i=0}^{L-1} s(i)\delta(t - iT_s)\right] * (h_{e1}(t) + h_{e2}(t)) + \widetilde{B}_{DC} + \widetilde{n}(t) \tag{3}$$

where, $h_{e1}(t) = \sqrt{\frac{P_t}{2}} R\mu G g_T(t) * l(t) * h_1(t) * g_R(t)$ and $h_{e1}(t) = \sqrt{\frac{P_t}{2}} R\mu G g_T(t) * l(t) * h_2(t) * g_R(t)$ are termed as the effective channel impulse response which includes effects of the propagation channel, front-ends and pulse shaping filter, $\widetilde{n}(t) = n(t) * g_R(t)$, $\widetilde{B}_{DC} = R\mu B_{DC} * l(t) * [h_1(t) + h_2(t)] * g_R(t)$.

Under the assumption of perfect synchronization and DC bias removal, the sampled version of the received electrical waveform, $r(t)$ can be given as,

$$r(i) = s(i)h_e(i) + \widetilde{n}(i) \tag{4}$$

where, $r(i)$, $\widetilde{n}(i)$ and $h_e(i) = h_{e1}(i) + h_{e2}(i)$ are the i^{th} sample of $r(t)$, $\widetilde{n}(t)$ and $h_e(t) = h_{e1}(t) + h_{e2}(t))$ respectively. Note that DC bias can be removed by using a DC blocker or by estimation. Here, we use a mini-circuit's DC blocker to remove the DC bias [19].

As depicted by the system model in Fig. 1, the received baseband signal samples from the USRP are first matched-filtered to improve the SNR. Subsequently, symbol synchronization is performed using the maximum output energy method [20], [21] to find the optimal sampling points of the symbols. The beginning of the frame is determined by cross-correlating the received frame with a clean copy of preamble sequence stored in the receiver. The location of the peak of the cross-correlator output is the beginning of the frame. The estimated channel DC gain is given by the average received channel estimation sequence. This is expressed as

$$\widehat{h}_e = \frac{1}{N_{CE}} \sum_{k=0}^{N_{CE}-1} r_{CE}(i) \tag{5}$$

where N_{CE} is the length of channel estimation sequence and $r_{CE}(i)$ is the received channel estimation sequence.

After channel estimation, the symbol decision can be obtained by a single tap equalizer given as

$$\widehat{s}(i) = r(i)(\widehat{h}_e)^{-1} \tag{6}$$

where $\widehat{h}_e$ is an average estimate of the effective optical DC channel coefficient. Now, we define the received electrical signal-to-noise ratio (SNR) as

$$SNR = \frac{\left|\widehat{h_e}\right|^2}{N_o} \tag{7}$$

where N_o is the estimated noise power which is obtained as power of received signal samples when no data is being transmitted.

III. Experimental System Design and Set-up

The experimental system set-up consists of one unit of Ettus USRP x310 and one unit of National Instruments USRP 2930. These USRPs are modified for baseband signal transmission/reception by replacing the default RF daughterboards with

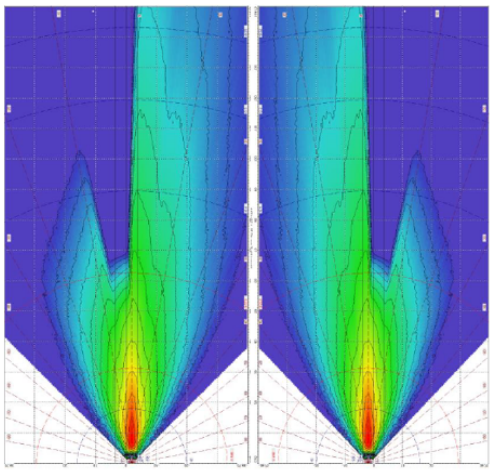

(a) LHL Pattern (b) RHL Pattern

Fig. 5: Ford F-MAX low beam headlight pattern

TABLE I: Specifications of Hardware Components

Component	Model	Specifications
Amplifier	Mini-circuits ZHL-32A+	0.05 to 130 MHz
LED Headlight	Ford F-MAX	2.3 MHz, 26 W
Photodetector (PD)	Thorlabs PDA100A2	10 MHz
USRP	x310/2930	0-30 MHz

baseband cards, that is, LFTX for transmission and LFRX for reception. Fig. 3 (a) and (b) depict the system block diagrams of the transmitter and receiver setups, respectively. On the transmitter side, a computer running LabVIEW is used to generate the transmit baseband signal according to the system model presented in Fig. 1. The baseband signal is fed to the USRP x310. The output analog signals from the two channels of USRP x310 are each amplified and fed to a custom-designed Bias-Tee which adds a 26.5 V DC signal to the message signal. The outputs of the bias tees are used to modulate two Ford F-MAX LED low-beam headlights, namely LHL and RHL.

At the receiver side, a single PD attached to the back of a preceding vehicle receives and converts the optical signal into an electrical signal. A mini-circuit DC blocker is used to filter out the DC component of the received signal before feeding it to the receive channel of the USRP 2930. The USRP 2930 shifts the signal to baseband, samples it and transfers the samples to a computer running LabVIEW program for baseband signal processing and data decoding. Table 1 lists the hardware components and related specifications of the experimental system.

IV. Measurement Results

The main system parameters of the experimental setup employed in the measurements are listed in Tables 1 and 2. In Fig. 5, we present the low-beam LED radiation patterns of the LHL and RHL used in the setup. The PD was attached to the center of the leading vehicle at a height of 60 cm from the ground. This point provided the maximum received

TABLE II: System Parameters

Parameter	Symbol	Value
Average Electrical Transmit Power	P_t	0 dB
Sampling Rate	F_s	2 MHz
Message Length	L	1024 bits
Upsample Factor	U	8
Data Rate	D	250 kbps
RRC Filter roll-off	α	0.3

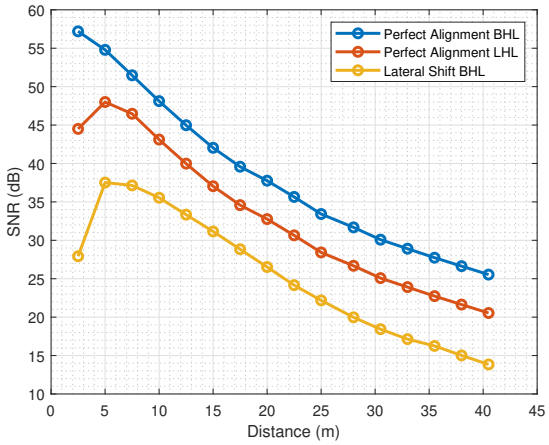

Fig. 6: SNR vs. distance measurement

Fig. 7: Google map image of test road track

power when both vehicles were perfectly aligned for the MISO configuration, which is consistent with the combined radiation pattern of both headlights presented in Fig. 5. Fig. 6 presents a plot of the received SNR versus distance when both vehicles are immobile. Three cases were considered for this study. The first case is a perfect alignment between both vehicles, with both headlights (BHL) transmitting simultaneously (see Fig. 4a), whereas in the second case, only one headlight is transmitting. The third case illustrates a scenario in which there is a lateral shift of 1.9 m (see Fig. 4b) between both vehicles with BHL transmitting. All measurements were performed at 2.5 m intervals. Owing to the limited space at the measurement facility, we measured up to 40 m. From the plot, we see that there is an SNR gain of approximately 5 dB when BHL is utilized to simultaneously transmit data, as compared to a single HL. After introducing the lateral shift, the SNR experienced a significant dip compared to when both vehicles were perfectly aligned.

Our next measurements sought to investigate the perfor-

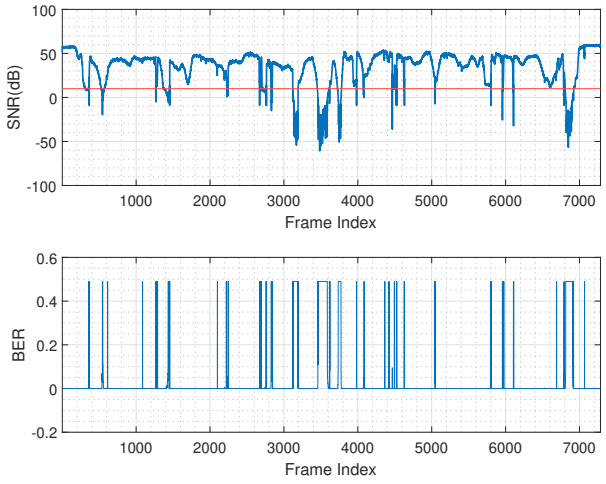

Fig. 8: SNR and BER during vehicle mobility for a round trip in 2x1 MISO configuration (trip 1)

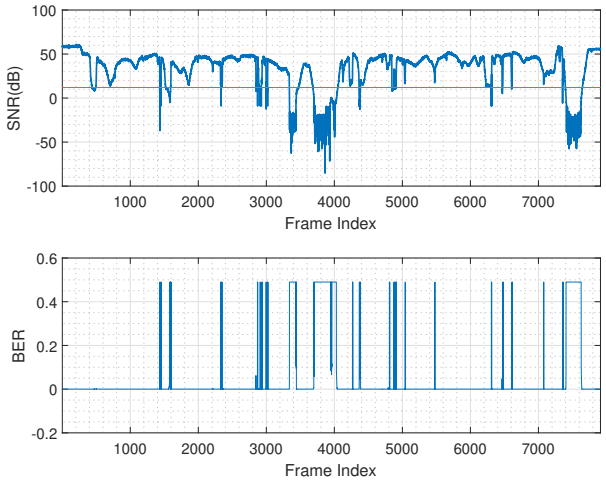

Fig. 9: SNR and BER during vehicle mobility for a round trip in 2x1 MISO configuration (trip 2)

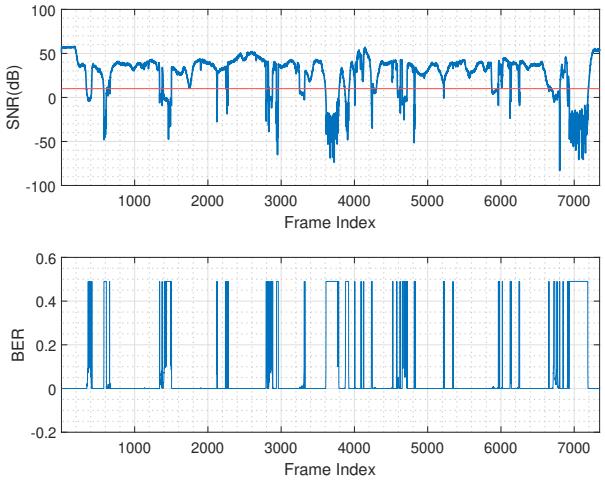

Fig. 10: SNR and BER during vehicle mobility for a round trip in SISO configuration (trip 1)

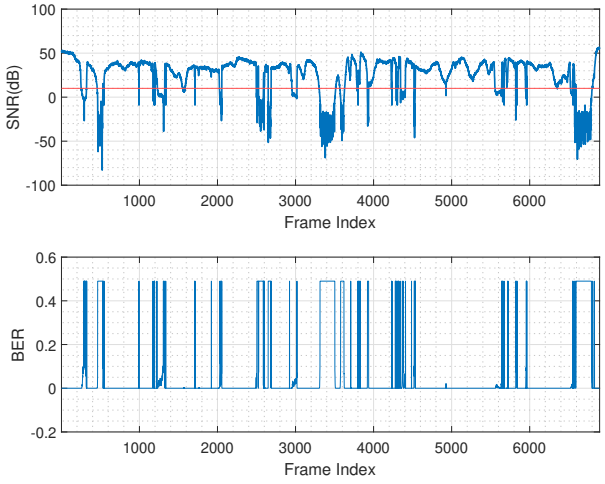

Fig. 11: SNR and BER during vehicle mobility for a round trip in SISO configuration (trip 2)

mance of the 2×1 MISO vehicular VLC system under mobility conditions. For this, we conducted vehicle mobility tests in which we drove the two vehicles on a road track on the Ozyegin university campus. Fig. 7 shows the road track for this experiment, which covers approximately 1 km of a round trip. The following and leading vehicles were separated by 8 -10 m, while driving at a speed of approximately 20 km/h. The red arrow indicates the driving route, which begins and ends at the tip of the red arrow for one trip. The experiment was conducted between the hours of 19:00 and 21:00 at night. Two scenarios were considered in the mobility tests. In the first scenario, BHL were transmitting simultaneously (2X1 MISO configuration) and in the second scenario, only the LHL is used to transmit signals to the PD (SISO configuration).

We present SNR and BER measurements of the packets received during the mobility test. The reliability of the system is given in terms of the packet delivery radio (PDR), a metric that defines the number of packets successfully delivered to the receiver [15]. Specifically, we defined a successfully delivered packet as a packet with received SNR greater than 10 dB. For OOK modulation, the BER at an SNR of 10 dB is below the forward error correction (FEC) limit of 3.8×10^{-3}, and such errors can be corrected by applying error control codes. Fig. 8 and 9 show the instantaneous SNR and BER per packet for round trips 1 and 2, respectively, for the 2×1 MISO configuration. Fig. 10 and 11 show the instantaneous SNR and

TABLE III: PDR under Vehicle Mobility

	MISO	SISO
Trip 1 PDR (%)	88.86	80.69
Trip 2 PDR (%)	90.31	81.42
Average PDR (%)	89.58	81.05

BER per packet for round trips 1 and 2, respectively, for the SISO configuration. The red horizontal line in the SNR plots indicates an SNR threshold of 10 dB, below which we consider packet delivery to be unsuccessful.

We observed that most packets were lost during a curve in the track as the SNR stayed longer below the threshold because of the reduced received optical power caused by misalignment between the headlights and the PD. Additionally, locations where the SNR falls below the threshold for a short period (a few frames) can be ascribed to road ramps, irregular and rough road surfaces, which cause sudden up and down movements in the position of the PD with respect to the ground. PDR of 88.86% and 90.31% are achieved for the first and second round trips of the 2×1 MISO scenario, respectively, which results in an average PDR of 89.58%. This decreased to 80.69% and 81.42% for the first and second round trips of the SISO scenario with an average PDR of 81.05%. Table 3 summarizes the PDRs. This performance gain of MISO over SISO is attributed to the link diversity provided by the two headlights, as well as the signal contribution received from both headlights.

V. Conclusion and future work

We presented an experimental investigation of an MISO vehicular VLC system implemented on a software-defined radio platform. The MISO system with repetition coding was compared with the SISO system, and we observed an increase of approximately 8% in the PDR in favor of the MISO system. Our mobility tests further revealed that a vehicular VLC system with a single PD cannot guarantee 100% link reliability under mobility conditions for safety-critical applications in future ITSs. As a result, our future work will focus on techniques to improve reliability by employing multiple PDs distributed on the vehicle to provide multiple reception points for the transmitted optical signal to reduce the effect of misalignment between both vehicles during mobility.

Acknowlegment

This work was funded by the European Union's Horizon 2020 research and innovation program under the Marie Skłodowska Curie grant agreement ENLIGHTEM No. 814215.

References

[1] https://www.who.int/news-room/fact-sheets/detail/road-traffic-injuries. Accessed: 17/08/2023.

[2] G. Karagiannis et al., "Vehicular Networking: A Survey and Tutorial on Requirements, Architectures, Challenges, Standards and Solutions," *in IEEE Communications Surveys & Tutorials*, vol. 13, no. 4, pp. 584-616, Fourth Quarter 2011, doi: 10.1109/SURV.2011.061411.00019.

[3] P. Papadimitratos, A. D. La Fortelle, K. Evenssen, R. Brignolo, and S. Cosenza, "Vehicular communication systems: Enabling technologies, applications, and future outlook on intelligent transportation," *IEEE Communications Magazine*, vol. 47, no. 11, pp. 84–95,2009.

[4] M. Uysal, Z. Ghassemlooy, A. Bekkali, A. Kadri, and H. Menouar, "Visible light communication for vehicular networking: Performance study of a V2V system using a measured headlamp beam pattern model," *IEEE Vehicular Technology Magazine*, vol. 10, no. 4, pp. 45–53, 2015.

[5] D. Karunatilaka, F. Zafar, V. Kalavally, and R. Parthiban, "LED Based Indoor Visible Light Communications: State of the Art," *IEEE Communications Surveys & Tutorials*, vol. 17, no. 3, pp. 1649–1678, Mar. 2015.

[6] P. H. Pathak, X. Feng, P. Hu, and P. Mohapatra, "Visible Light Communication, Networking, and Sensing: A Survey, Potential and Challenges," *IEEE Communications Surveys & Tutorials*, vol. 17, no. 4, pp. 2047–2077, Feb. 2015.

[7] L. E. M. Matheus, A. B. Vieira, L. F. M. Vieira, M. A. M. Vieira, and O. Gnawali, "Visible Light Communication: Concepts, Applications and Challenges," *IEEE Communications Surveys & Tutorials, vol.* 21, no. 4, pp. 3204–3237, 2019.

[8] M. M. Céspedes, B. G. Guzmán, V. P. Gil Jiménez and A. G. Armada, "Aligning the Light for Vehicular Visible Light Communications: High Data Rate and Low-Latency Vehicular Visible Light Communications Implementing Blind Interference Alignment," *in IEEE Vehicular Technology Magazine*, vol. 18, no. 1, pp. 59-69, March 2023, doi: 10.1109/MVT.2022.3228389.

[9] H. Y. Tseng, Y. L. Wei, A. L. Chen, H. P. Wu, H. H. and H. M. Tsai, "Characterizing link asymmetry in vehicle-to-vehicle Visible Light Communications," *2015 IEEE Vehicular Networking Conference (VNC)*, Kyoto, 2015, pp. 88-95, doi: 10.1109/VNC.2015.7385552.

[10] M. S. Amjad et al., "An IEEE 802.11 Compliant SDR-Based System for Vehicular Visible Light Communications," *ICC 2019 - 2019 IEEE International Conference on Communications (ICC)*, Shanghai, China, 2019, pp. 1-6, doi: 10.1109/ICC.2019.8761960.

[11] M. S. Amjad et al., "Towards an IEEE 802.11 Compliant System for Outdoor Vehicular Visible Light Communications," *in IEEE Transactions on Vehicular Technology*, vol. 70, no. 6, pp. 5749-5761, June 2021, doi: 10.1109/TVT.2021.3075301.

[12] B. Aly, M. Elamassie and M. Uysal, "Vehicular VLC Channel Model for a Low-Beam Headlight Transmitter," *2021 17th International Symposium on Wireless Communication Systems (ISWCS)*, Berlin, Germany, 2021, pp. 1-5, doi: 10.1109/ISWCS49558.2021.9562187.

[13] B. Aly, M. Elamassie, and M. Uysal, "Vehicular vlc system with selection combining," *IEEE Transactions on Vehicular Technology,* vol. 71, no. 11, pp. 12 350–12 355, 2022.

[14] T. Saito, S. Haruyama and M. Nakagawa, "A New Tracking Method using Image Sensor and Photo Diode for Visible Light Road-to-Vehicle Communication," *2008 10th International Conference on Advanced Communication Technology*, Gangwon, Korea (South), 2008, pp. 673-678, doi: 10.1109/ICACT.2008.4493850.

[15] S. Okada, T. Yendo, T. Yamazato, T. Fujii, M. Tanimoto and Y. Kimura, "On-vehicle receiver for distant visible light road-to-vehicle communication," *2009 IEEE Intelligent Vehicles Symposium*, Xi'an, China, 2009, pp. 1033-1038, doi: 10.1109/IVS.2009.5164423.

[16] D. K. Tettey, M. Elamassie, and M. Uysal, "Experimental Investigation of Angle Diversity Receiver for Vehicular VLC," *In Proc. of the 29th Annual International Conference on Mobile Computing and Networking (ACM MobiCom)*, Madrid, Spain, Oct. 2023.

[17] H. B. Eldeeb, S. M. Sait, and M. Uysal, "Visible light communication for connected vehicles: How to achieve the omnidirectional coverage?" *IEEE Access*, vol. 9, pp. 103 885–103 905, 2021.

[18] W. -H. Shen and H. -M. Tsai, "Testing vehicle-to-vehicle visible light communications in real-world driving scenarios," 2017 IEEE Vehicular Networking Conference (VNC), Turin, Italy, 2017, pp. 187-194, doi: 10.1109/VNC.2017.8275596.

[19] https://www.mouser.com.tr/new/mini-circuits/mini-circuits-blk89s-plus-dc block/? Accessed: 14/09/2023

[20] R. W. H. Jr., *Introduction to Wireless Digital Communication: A Signal Processing Perspective*, Englewood Clifs, NJ, USA: Prentice-Hall, Mar. 2017.

[21] B. Aly, M. Elamassie, B. Kebapci and M. Uysal, "Experimental Evaluation of a Software Defined Visible Light Communication System," *2020 IEEE International Conference on Communications Workshops (ICC Workshops)*, Dublin, Ireland, 2020, pp. 1-6, doi: 10.1109/ICCWorkshops49005.2020.9145145.